

# Consolidation of Calcium Phosphate Powder Through Microwave Sintering

Natasha Ahmad Nawawi<sup>1\*</sup>, Ramesh Singh<sup>2</sup>, Tan Chou Yong<sup>2</sup>

<sup>1</sup>Fakulti Kejuruteraan Mekanikal, Universiti Teknologi Mara Cawangan Pulau Pinang, Kampus Permatang Pauh, Jalan Permatang Pauh, 13700 Perai, Pulau Pinang.

<sup>2</sup>Department of Mechanical Engineering, University of Malaya, 50603 Kuala Lumpur, Wilayah Persekutuan.

\*corresponding author: natashanawawi@uitm.edu.my

---

## ARTICLE HISTORY

## ABSTRACT

Received  
2 October 2018

Accepted  
19 November 2018

Available online  
30 December 2018

*In the last 50 years, the major drawback of HA ceramic usage in clinical applications is its inherent brittleness and lower mechanical strength than those of cortical bone. This is turn calls for the development of dense nanostructured HA with the major concern is to enhance densification while limiting its grain growth. Hence, a promising way to obtain this could be a fabrication of fully dense nanostructured materials through sintering process. In this work, eggshell derived hydroxyapatite (HA-Es) powder has been prepared via solid state sintering and its sinterability was investigated through microwave sintering at various sintering temperatures (950-1250 °C). The phase stability, microstructural evolution and relative density of HA-Es were deliberated. The results indicate that microwave sintering regime has been successfully employed and this short sintering regime did not promote extensive grain growth even when sintered at high temperature.*

**Keywords:** calcium phosphate, synthesis, solid state sintering, microwave sintering, microstructure

## 1. INTRODUCTION

Hydroxyapatite (HA) with the chemical composition of  $\text{Ca}_{10}(\text{PO}_4)_6(\text{OH})_2$ , is the most significant among the calcium phosphate compounds as its composition is found close to the dominant inorganic component of human body hard tissues such as bone, dentin and enamel. Mineral component of bone is composed of nanostructured non-stoichiometric HA of dimensions 20 nm in diameter and 50 nm long with trace amounts of ions such as  $\text{Na}^+$ ,  $\text{Mg}^{2+}$ ,  $\text{K}^+$ ,  $\text{F}^-$  and  $\text{CO}_3^{2-}$ . Besides being non-toxic, one of the outstanding hydroxyapatite properties as a biomaterial is its excellent biocompatibility which originated from its similarity in chemical composition to hard tissue. It also appears to promote and form a direct chemical bonding with bone (bioactive) [1-2]. It was also reported that the mineral part of bone and teeth is made of a crystalline form of calcium phosphate that is similar to HA [3]. Hence, HA in the nanocrystalline form is usually applied for implant coatings, dental cements and dental toothpastes due to a high bioactivity characteristic of this compound [4].

However, the inherent brittleness and low mechanical strength, i.e. lower toughness ( $0.8-1.2 \text{ MPam}^{1/2}$ ) and flexural strength ( $< 140 \text{ MPa}$ ) than those of human cortical bone [5] limits its application to the non-load bearing areas. Moreover, the poor mechanical behaviour is more obvious for highly porous ceramics and scaffolds due to the conflicting requirements of porosity and strength [6]. However, its preparation with superior mechanical properties is possible if the starting HA powder is stoichiometry, i.e. has Ca/P molar ratio of 1.67. Moreover, mechanical strength and bioactivity of HA depend strongly upon its microstructure such as grain size and distribution, porosity and its shape and distribution, and material crystallinity [1]. Therefore,

with proper designing and processing, the HA with improved and desired properties could be prepared.

Conventionally, HA ceramics bodies are produced via compaction of HA powder followed by sintering of the compacted HA green bodies at predetermined temperature and soaking time in air atmosphere. This final step consists of elimination of pores and induces consolidation and densification of the compacted body through thermal treatment at high temperature that is lower than the melting point [7]. The most popular consolidation technique used is the conventional pressureless sintering. However, long sintering hours usually result in coarse-grained microstructure and low mechanical properties. In general, consolidation of ceramic through conventional method requires high sintering temperatures and long sintering times which often result in grain coarsening and decomposition of the HA phase, which in turn results in deterioration of the mechanical properties of ceramic [8-9]. For example, sintering above 1300 °C was reported to introduce secondary phases of calcium phosphates such as CaO and  $\alpha$ -TCP [10].

Consequently, microwave sintering (MS) of ceramics has gained much attention during the last decade. Since heat is generated within the material, rapid and uniform heating are achievable followed by enhanced densification rate, improved microstructure and potential for energy and cost savings when compared to conventional sintering [11]. For microwave sintering, there are 3 vital parameters that need to be controlled which include sintering temperature, heating rate and holding time. In a reported literature, it was affirmed that too high sintering temperature (1200 °C), long holding time (3 min) or slow heating rate (30 °C/min) directed the growth of HA nanoparticles into the microscale grains [12]. Contrary to this, at a lower sintering temperature (i.e. 950 °C) it was found that the nanoparticles grains did not fuse completely and formed a rougher surface in the microscale region. In another research performed based on the effect of microwave and conventional sintering on HA, the authors reported that the density of microwave sintered samples was in the range ~95.6 – 98.8 % of theoretical density [13]. However, conventional samples attained densification in the range of ~93.8 – 97.9 % of theoretical density. Furthermore, the authors found that microwave sintered samples have finer grain size than conventional sintered samples which led to greater densification of microwave sintered HA samples [13]. Hence, the selection of suitable sintering method is a critical controlling parameter to produce HA with desired structure and properties. The present research aims at producing sinterability studies of nanostructured calcium phosphate ceramics derived from natural sources by using waste eggshells as a calcium precursor via microwave sintering. Further characterization was then performed to evaluate the effect of various microwave sintering temperature on the phase stability, microstructure evolution and mechanical properties of the derived HA compacts.

## 2. MATERIALS AND METHODS

### *2.1 Preparation of HA powder using waste eggshell as a calcium precursor*

In this work, phase pure HA was synthesized via solid state reaction method as described in the previous work [14]. Calcium carbonate ( $\text{CaCO}_3$ ) from waste eggshell was used as a source of calcium precursor to synthesize HA. The calcined eggshell was added to phosphorus precursor, calcium hydrogen phosphate dehydrate,  $\text{CaHPO}_4 \cdot 2\text{H}_2\text{O}$  (DCPD, Nacalai Tesque, Japan) at a Ca/P ratio of 1.67 and this mixture is subjected to attrition milling (Akron Electric Inc., USA) at a speed of 400 rpm for 2 hours. The obtained powder mixture was dried in the oven overnight.

The dried powder is sieved through the 212  $\mu\text{m}$  mesh to obtain a fine powder. In short, the HA derived from eggshell was referred to as HA-Es.

## ***2.2 Preparation of HA-Es green bodies for microwave sintering***

The synthesized HA-Es powder was uniaxially compacted at 15 MPa into circular disc samples. The green compacts were subsequently subjected to cold isostatic pressing and the consolidation of the particles was performed using microwave sintering furnace (Shenzen BduVo, Delta, China) within a temperature range of 950-1250  $^{\circ}\text{C}$  for 15 minutes and subsequently left to furnace cool. The operating power of the microwave system was optimized through several trials runs and finally, it was set to an operation to avoid overheating and cracking of samples. Power was provided by a 6-kW magnetron which is controlled by a programmable process controller. The sintered samples were then ground using silicon carbide (SiC) sand papers and polished to a 1  $\mu\text{m}$  mirror finish using diamond paste as a polishing medium prior to evaluation. The microwave sintered HA compacts are then termed as HA-Es(M). The general observation was that HA-Es(M) samples did not show any sign of cracking after sintering regardless the high heating rate that was employed during microwave sintering.

## ***2.3 Physical and chemical characterization of HA-Es sintered samples***

All sintered HA compacts were characterized for their phase purity and stability using X-ray diffractometer (XRD) (PANalytical, Empyrean diffractometer, Netherlands) while the powder size and morphology were characterized using Scanning Electron Micrographs (SEM) (Phenom Pro X, Netherlands). In the present work, the crystalline phase present in the material was identified by comparing the prominent XRD peaks exhibited by the material tested to that of standard reference JCPDS-ICCD (Joint Committee of Powder Diffraction Standard-International Centre for Diffraction Data).

Subsequently, these HA compacts were tested to determine effect of different sintering temperature on its microstructural evolution and mechanical properties (relative density, Vickers hardness and fracture toughness). The grain size of sintered HA compacts was determined from SEM images based on the linear intercept method in accordance with ASTM E112-96 standard. The bulk density of the sintered samples was measured after sintering at various temperature and time using a water immersion technique which was based on the Archimedes method. Meanwhile, the linear shrinkage is determined based on their length measurement of the cold isostatically pressed bar samples before and after sintering under standard conditions. It is customary to express shrinkage (or growth) as a percentage of sintered length.

$$\text{Shrinkage (or growth) \%} = \frac{\text{change in length}}{\text{sintered length}} * 100$$

## **3. RESULTS AND DISCUSSION**

The XRD phase analysis of the HA-Es(M) compacts sintered at varying temperatures is presented in Figure 1. The XRD traces indicate that the phase stability of HA-Es powder compacts was not disrupted by microwave sintering up to 1200  $^{\circ}\text{C}$  as all major peaks of pure HA (JCPDS: 00-009-0432) was detected. However, sintering at 1250  $^{\circ}\text{C}$  resulted in decomposition of the HA phase to form small amounts of  $\beta$ -TCP (JCPDS: 00-009-0169) and

$\alpha$ -TCP (JCPDS: 00-009-0348). This was reflected by the decrease in the intensity of the (211) lattice plane at  $2\theta \sim 31.77^\circ$  at  $1250^\circ\text{C}$  which was initially increasing from  $950^\circ\text{C}$  to  $1200^\circ\text{C}$ . Moreover, this observation corresponded to the reported literature where high temperature sintering of HA led to the partial thermal decomposition of HA into TCP and/or TTCP [15]. Similarly, such decomposition to  $\beta$ -TCP together with CaO at  $1250^\circ\text{C}$  has also been reported in the sinterability study of eggshell derived HA powder through microwave sintering [16]. However, in this work the presence of CaO phase was not detected throughout the sintering regime which was similar to the behavior of HA-Es samples sintered through conventional sintering [14]. This finding has somehow highlighted the advantage of the eggshell derived HA through solid state reaction. Note that, CaO is formed during sintering if the Ca/P molar ratio of the HA exceeds the value of 1.67 [16-17]. The presence of CaO is not favored in HA phase as it is found to be toxic to biological cells and detrimental to the mechanical properties. In addition, it was reported that the existence of CaO in HA would decrease the strength due to the stresses developed in the matrix because of a change in volume associated with the formation of  $\text{Ca}(\text{OH})_2$  [18]. Indirectly, this indicates that the HA-Es powder synthesized in this present work has a better phase stability compared to the reported literature [16].

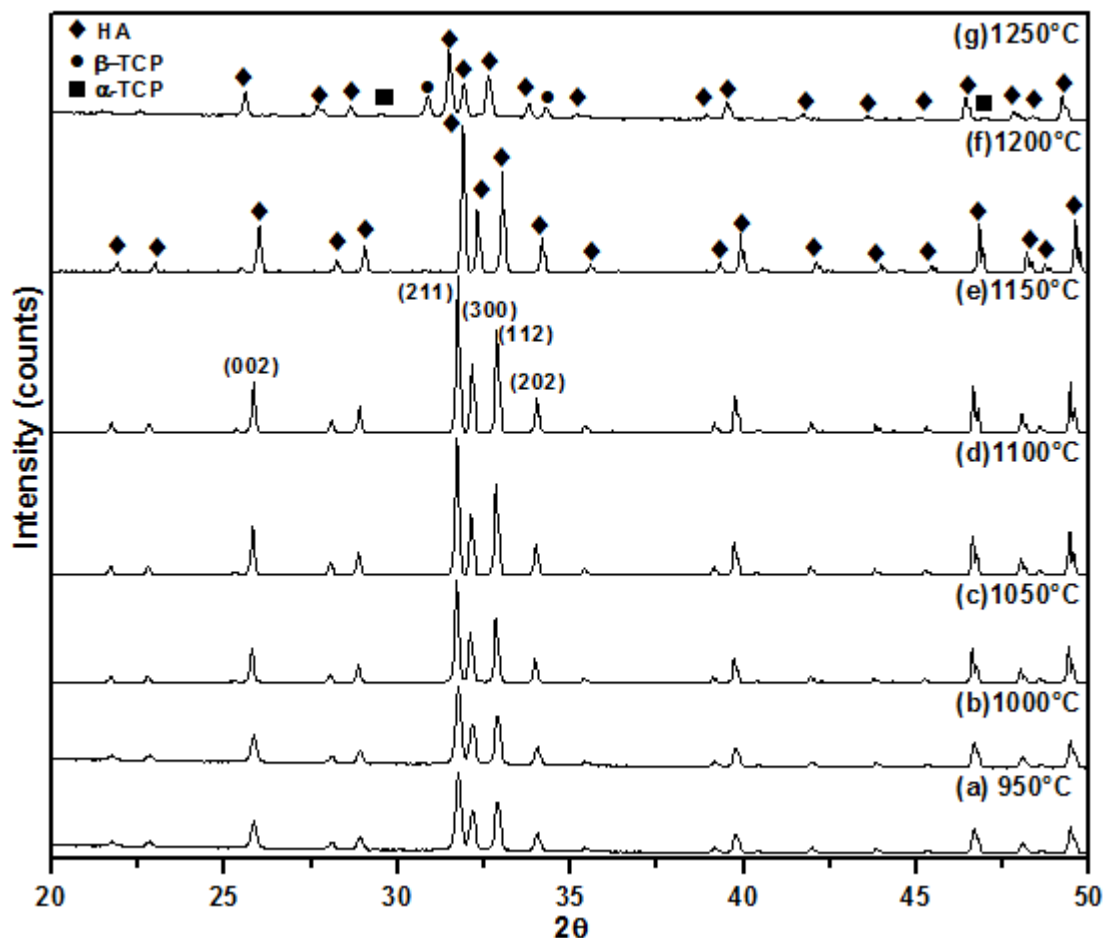


Figure 1: XRD patterns of HA-Es(M) samples microwave-sintered at various temperatures

It was claimed that thermal decomposition takes place through two stages that are dehydroxylation and decomposition, and this occurrence could be observed by comparing the

XRD peaks position of the sintered material to the standard JCPDS data for stoichiometric HA [19]. In Figure 1, it can be visually seen that the peak shifting of HA-Es(M) was not visible at the three main lattice planes of HA; (211) at  $31.77^\circ$ , (300) at  $32.90^\circ$  and (112) at  $32.20^\circ$ ; from  $950^\circ\text{C}$  to  $1200^\circ\text{C}$ , except at  $1250^\circ\text{C}$ . The peak shifting for HA-Es(M) was found to vary between  $0.04^\circ - 0.07^\circ$ . This observation is in line with the hypothesis claimed in the reported literature [19].

The linear shrinkage based on the measurement of the bar samples for HA-Es(M) with respect to sintering temperature is shown in Figure 2. There was no sign of cracking observed in any of the HA-Es samples. In general, the results indicate that the HA-Es(M) exhibits a gradual increase in linear shrinkage from 1.0 % to 16.2 %. It is known that prior calcination treatment on HA powder delays the initiation of sintering. It was reported that for calcination at  $800^\circ\text{C}$  and above, the shrinkage rate decreases, therefore, higher temperature is necessary to reach the final stage of sintering [20]. Meanwhile, for non-calcined and calcined at  $700^\circ\text{C}$  samples, it was reported that the sintering start to begin at a lower temperature and higher temperature is needed for pore diminishing in the final sintering stage, hence, there is a tendency for grain growth to take place simultaneously [20]. In this current work, HA-Es powder was calcined at  $800^\circ\text{C}$  during the preparation of the powder, hence, it is expected for the HA-Es to exhibit lower linear shrinkage and smaller grain growth.

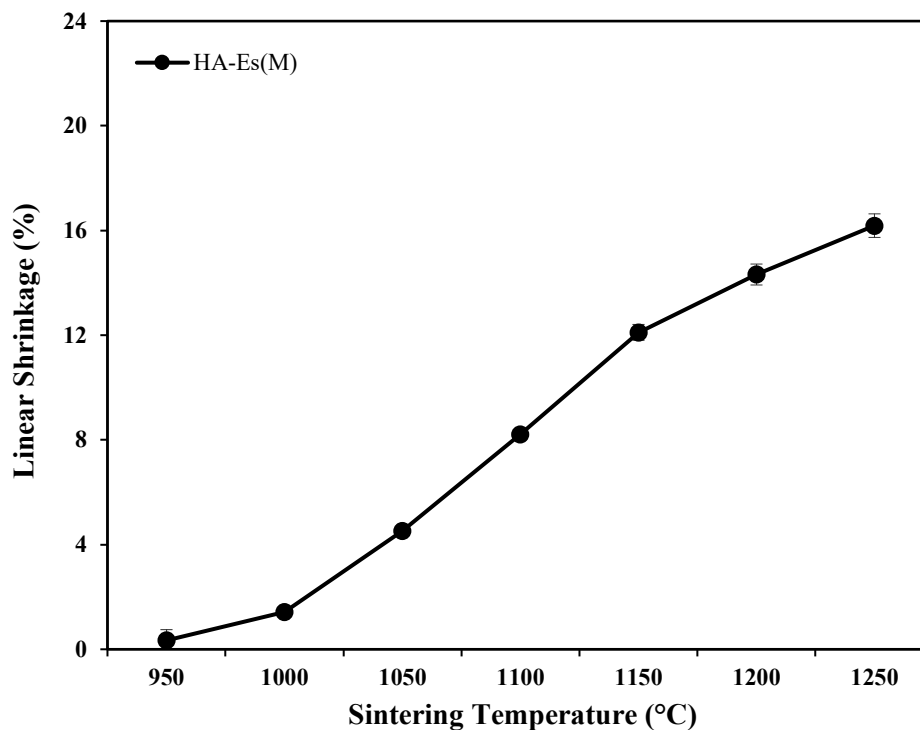
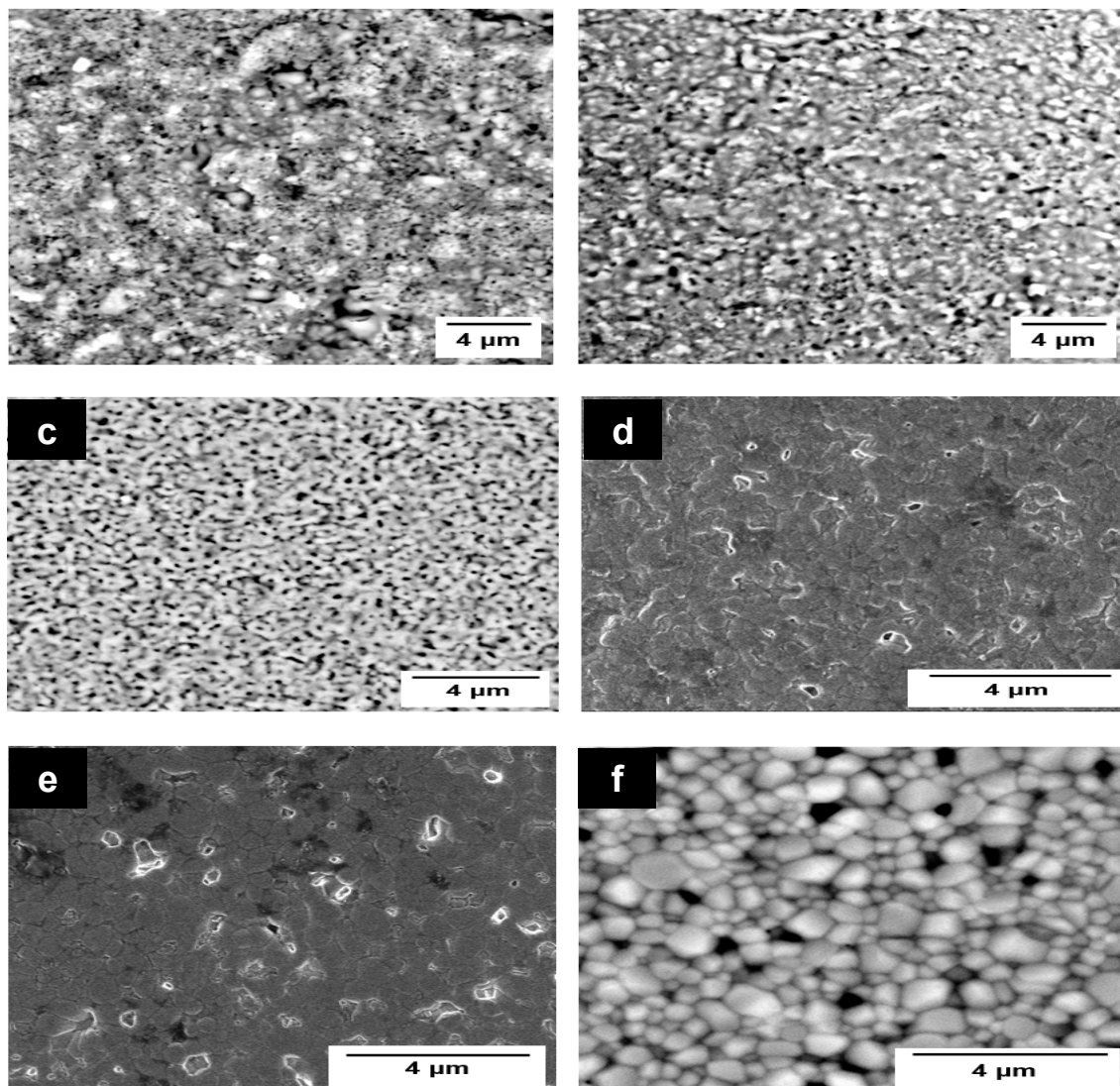


Figure 2: Linear shrinkage of HA-Es(M) samples microwave-sintered at various sintering temperatures

The microstructural evolution of the HA-Es(M) sintered at various temperatures is presented in Figure 3. In Figure 3 (a), the micrograph consists of a fine mixture of petal-like flakes structure of the HA-Es agglomerates which are still intact with slightly deformed agglomerates. Roughly it can be seen that there was no bonding formed between the flowers like agglomerates at the

low microwave sintering temperature of 950 °C. However, the HA-Es agglomerates have fused and bond with adjacent particles with increased interconnected porosity due to surface diffusion at a sintering temperature of 1000 °C. At 1050 °C, the neck formations between the agglomerated particles had taken place and at this stage, the microstructure was characterized by spherical and shapeless inter-agglomerate pores. As the sintering temperature increased to 1100 °C, the small particulate phase was widely distributed across the surface of the grain boundaries and within the grains [21]. Therefore, stronger bonds between the agglomerates were formed. The average grain size was measured to be  $750 \pm 0.05$  nm.



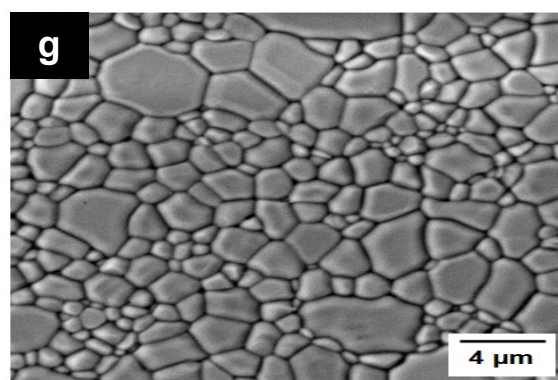


Figure 3: Microstructural evolution of HA-Es(M) samples microwave-sintered at (a)950 °C, (b)1000 °C, (c)1050 °C, (d)1100 °C, (e)1150 °C, (f)1200 °C and (g)1250 °C

Meanwhile at 1150 °C, HA-Es(M) exhibits more uniform microstructure, fewer intergranular pores and accompanied by grain coarsening with a slight increase in average grain size to  $850\pm 0.04$  nm. At 1200 °C, grain growth has started as the average grain size has tremendously increased by a factor of 2.4 to  $2.08\pm 0.04$   $\mu\text{m}$ . Note that, at this sintering temperature phase decomposition to TCP has taken place and beyond this point, the greater portion of HA-Es(M) had been transformed to  $\beta$ -TCP and  $\alpha$ -TCP as seen in Figure 1. The grain size was found to increase by a factor of 1.1 to  $2.28\pm 0.06$   $\mu\text{m}$  when the temperature increased by 50 °C from 1200 °C. In addition, this result is in line with the lower linear shrinkage result obtained for HA-Es(M) sintered compacts (Figure 2), which indicates that higher sintering temperature is needed for maximum densification. This is because the synthesized HA-Es powder was calcined prior to its compaction, hence less probability of a rapid grain growth as the sintering rate was reduced due to larger powder particle size [22]. On top of all, these results indicate that microwave sintering regime employed did not promote extensive grain growth even when sintered at high temperature. This is proven by the nanostructure (less than 1  $\mu\text{m}$ ) exhibited by their SEM images even when sintered at 1150 °C as shown in Figure 3(e). In addition, the lower grain growth exhibited by HA-Es(M) could also reflect the lower densification achieved in these samples. Thus, it is believed that the grain boundary diffusion through the densification mechanism does not reach a densification level which is conducive to grain growth.

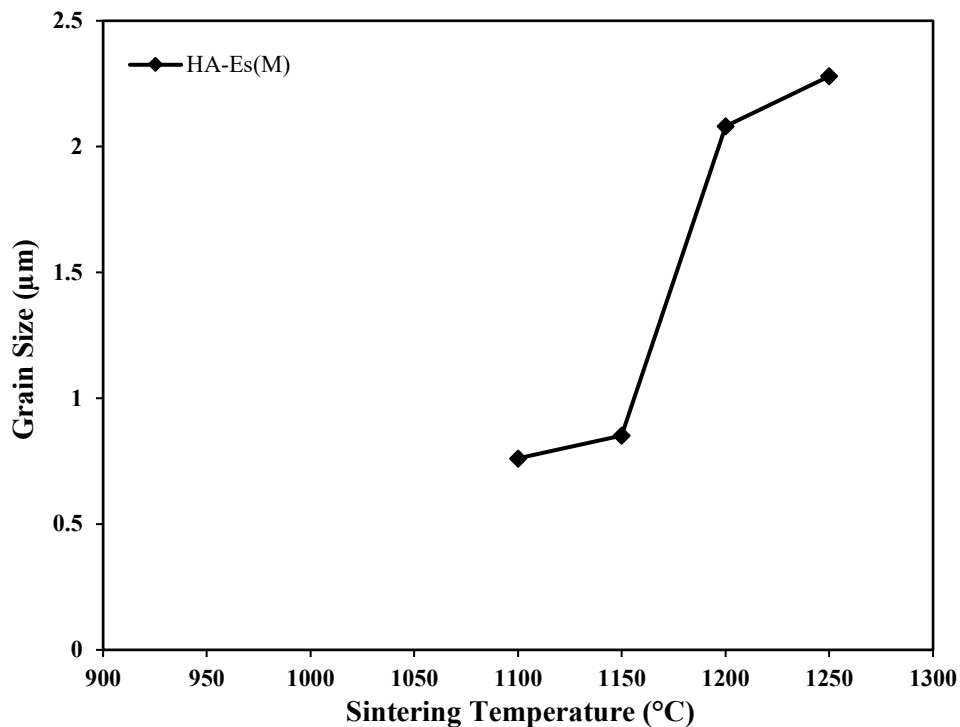


Figure 4: Average grain size variation of HA-Es(M) and HA-Wp(M) samples microwave-sintered at various temperatures

The effect of microwave sintering on the densification of HA pellets as a function of sintering temperatures is shown in Figure 5. The steady increase in bulk density variation corresponds well with a densely packed microstructure of sintered HA-Es with the increasing sintering temperature as shown in the SEM images in Figure 3. The onset of densification for HA-Es(M) which is shown by the sharp increase in the sintered density has taken place between 1050 °C to 1100 °C. The HA-Es(M) ceramic exhibited a lower value of 92.4 % at 950 °C to 92.8 % when sintered at 1000 °C. The relative density increased from 93.1 % at 1050 °C to above 95 % of theoretical density value when sintered at 1150 °C. The maximum value of 97.1 % was attained for compacts that were sintered at 1250 °C. However, the maximum value of relative density achieved by HA-Es(M) compacts at 1250 °C are in good agreement to the density of biphasic mixture phase (HA and TCP) as HA-Es have decomposed to secondary phases at 1250 °C. This apparent increase, in this case, might be due to the allotropic transformation of HA to  $\beta$ -TCP which has a lower theoretical density of 3.07 g/cm<sup>3</sup> [16]. In fact, the lower grain growth exhibited by HA-Es(M) samples as in Figure 4, indirectly reflects the lower level of densification obtained by the samples. This was also supported by the linear shrinkage result obtained for HA-Es(M) sintered compacts (Figure 2) as higher sintering temperature is necessary for maximum densification.

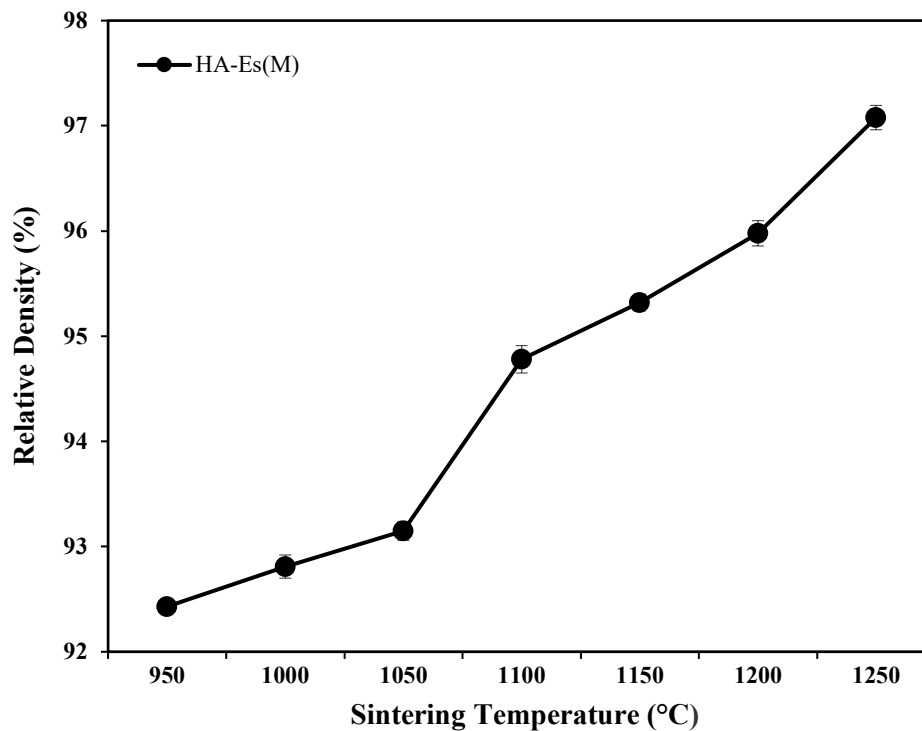


Figure 5: The variation in relative density of microwave sintered HA-Es(M) as a function of sintering temperature

#### 4. CONCLUSION

The sintering process of the HA powders through microwave sintering at various sintering temperatures (950-1250 °C) revealed that the decomposition of HA-Es(M) to  $\beta$ -TCP and  $\alpha$ -TCP has taken place beyond 1200 °C and the maximum HA-Es(M) relative density of 97.1 % was attained at 1250 °C. Besides that, the porosity on the samples surface has led to lower densification level hence lowering the linear shrinkage. Moreover, it was proven in this work that the sintering regime applied did not promote extensive grain growth even when sintered at a high temperature. Based on the results, the effectiveness of microwave sintering can be noted as higher density can be achieved at all temperatures within the shorter sintering time than any conventional pressureless sintering method.

#### ACKNOWLEDGEMENT

The authors would like to acknowledge University Teknologi Mara and University of Malaya, Malaysia for providing the necessary facilities and resources for this research.

#### REFERENCES

- [1] K. Ishikawa, S. Matsuya, Y. Miyamoto, and K. Kawate, "9.05-Bioceramics," *Comprehensive Structural Integrity*, pp. 169-214, 2003.

- [2] S. V. Dorozhkin, "Bioceramics of calcium orthophosphates," *Biomaterials*, vol. 31(7), pp. 1465–1485, 2010.
- [3] J. Park and R. S. Lakes, "*Biomaterials: an introduction*," Springer Science & Business Media, 2007.
- [4] D. L. Goloshchapov, V. M. Kashkarov, N. A. Rumyantseva, P. V. Seredin, A. S. Lenshin, B. L. Agapov, and E. P. Domashevskaya, "Synthesis of nanocrystalline hydroxyapatite by precipitation using hen's eggshell," *Ceramics International*, vol. 39(4), pp. 4539–4549, 2013.
- [5] S. V. Dorozhkin, "Nanosized and nanocrystalline calcium orthophosphates," *Acta Biomaterialia*, vol. 6(3), pp. 715–734, 2010.
- [6] B. D. Ratner, A. S. Hoffman, F. J. Schoen, and J. E. Lemons, "*Biomaterials science: an introduction to materials in medicine*," Academic Press, 2004.
- [7] E. Champion, "Sintering of calcium phosphate bioceramics," *Acta Biomaterialia*, vol. 9(4), pp. 5855–5875, 2013.
- [8] Y. W. Gu, K. A. Khor, and P. Cheang, "Bone-like apatite layer formation on hydroxyapatite prepared by spark plasma sintering (SPS)," *Biomaterials*, vol. 25(18), pp. 4127–4134, 2004.
- [9] C. Y. Tang, P. S. Uskokovic, C. P. Tsui, D. Veljovic, R. Petrovic, and D. Janackovic, "Influence of microstructure and phase composition on the nanoindentation characterization of bioceramic materials based on hydroxyapatite," *Ceramics International*, vol. 35(6), pp. 2171–2178, 2009.
- [10] D. Tadic, F. Beckmann, K. Schwarz, and M. Epple, "A novel method to produce hydroxyapatite objects with interconnecting porosity that avoids sintering," *Biomaterials*, vol. 25(16), pp. 3335–3340, 2004.
- [11] A. Harabi, D. Belamri, N. Karboua, and F. Z. Mezahi, "Sintering of bioceramics using a modified domestic microwave oven: Natural hydroxyapatite sintering," *Journal of Thermal Analysis and Calorimetry*, vol. 104(1), pp. 383–388, 2011.
- [12] Y. Hong, H. Fan, B. Li, B. Guo, M. Liu, and X. Zhang, "Fabrication, biological effects, and medical applications of calcium phosphate nanoceramics," *Materials Science and Engineering R: Reports*, vol. 70(3-6), pp. 225–242, 2010.
- [13] Yang, Y., Ong, J. L., & Tian, J. (2002). Rapid sintering of hydroxyapatite by microwave processing. *Journal of Materials Science Letters*, 21(1), 67–69.
- [14] S. Ramesh, A. N. Natasha, C. Y. Tan, L. T. Bang, S. Ramesh, C. Y. Ching, and Hari Chandran, "Direct conversion of eggshell to hydroxyapatite ceramic by a sintering method," *Ceramics International*, vol. 42, pp. 7824–7829, 2016.
- [15] S. Ramesh, C. Y. Tan, S. B. Bhaduri, W. D. Teng, and I. Sopyan, "Densification behaviour of nanocrystalline hydroxyapatite bioceramics," *Journal of Materials Processing Technology*, vol. 206(1-3), pp. 221–230, 2008.
- [16] D. S. R. Krishna, A. Siddharthan, S. K. Seshadri, and T. S. Kumar, "A novel route for synthesis of nanocrystalline hydroxyapatite from eggshell waste," *Journal of Materials Science: Materials in Medicine*, vol. 18(9), pp. 1735–1743, 2007.
- [17] W. Suchanek and M. Yoshimura, "Processing and properties of hydroxyapatite-based biomaterials for use as hard tissue replacement implants," *Journal of Materials Research*, vol. 13(01), pp. 94–117, 1998.
- [18] M. A. Fanovich and J. M. Porto-Lopez, "Influence of temperature and additives on the microstructure and sintering behaviour of hydroxyapatites with different Ca/P ratios," *Journal of Materials Science: Materials in Medicine*, vol. 9(1), pp. 53–60, 1998.
- [19] Y. W. Gu, N. H. Loh, K. A. Khor, S. B. Tor, and P. Cheang, "Spark plasma sintering of hydroxyapatite powders," *Biomaterials*, vol. 23(1), pp. 37–43, 2002.
- [20] H. Y. Juang and M. H. Hon, "Effect of calcination on sintering of hydroxyapatite," *Biomaterials*, vol. 17(21), pp. 2059–2064, 1996.
- [21] A. Chanda, S. Dasgupta, S. Bose, and A. Bandyopadhyay, "Microwave sintering of calcium phosphate ceramics," *Materials Science and Engineering C*, vol. 29(4), pp. 1144–1149, 2009.
- [22] C. Kothapalli, M. Wei, A. Vasiliev, and M. T. Shaw, "Influence of temperature and concentration on the sintering behaviour and mechanical properties of hydroxyapatite," *Acta Materialia*, vol. 52(19), pp. 5655–5663, 2004.